

Coexistence of Itinerant Electrons and Local Moments in Iron-Based Superconductors

Su-Peng Kou¹, Tao Li², and Zheng-Yu Weng^{3*}

¹*Department of Physics, Beijing Normal University, Beijing, 100875, China*

²*Department of Physics, Renmin University of China, Beijing, 100872, China*

³*Center for Advanced Study, Tsinghua University, Beijing, 100084, China*

(Dated: February 21, 2024)

In view of the recent experimental facts in the iron-pnictides, we make a proposal that the itinerant electrons and local moments are simultaneously present in such multiband materials. We study a minimal model composed of coupled itinerant electrons and local moments to illustrate how a consistent explanation of the experimental measurements can be obtained in the leading order approximation. In this mean-field approach, the spin-density-wave (SDW) order and superconducting pairing of the itinerant electrons are not directly driven by the Fermi surface nesting, but are mainly induced by their coupling to the local moments. The presence of the local moments as independent degrees of freedom naturally provides strong pairing strength for superconductivity and also explains the normal-state linear-temperature magnetic susceptibility above the SDW transition temperature. We show that this simple model is supported by various anomalous magnetic properties and isotope effect which are in quantitative agreement with experiments.

PACS numbers: 74.20.Mn, 71.27+a, 75.20.Hr

I. INTRODUCTION

Since the discovery of superconductivity (SC) in iron pnictides¹⁻⁵, with T_c being quickly raised to 55 K⁵, intensive attentions have been focused on possible underlying mechanisms. With the neutron scattering measurement^{6,7} subsequently establishing the fact that an SDW order exists in the undoped LaOFeAs compound below $T_{\text{SDW}} \simeq 134$ K, which has been later generically found in other iron pnictides⁸⁻¹¹, the interplay between SC and antiferromagnetism (AF) has become a central issue.

The iron $3d$ -electrons are believed quite itinerant with their hybridized multi-orbitals forming multiple Fermi pockets at the Fermi level¹³. Many theoretical efforts^{12-14,17-21} are based on itinerant approaches in searching for possible SDW and SC mechanisms responsible for the iron pnictides. This kind of theory is generally sensitive to the detailed band structure where the Fermi surface nesting effect is important. As shown by a renormalization group analysis²¹, such an itinerant model does possess the instabilities towards the SDW and SC orderings. However, how to reach high- T_c in the SC phase and at the same time have a self-consistent description of the magnetic phase within a unified framework remains a challenge.

Alternatively local moment descriptions have been also promoted²²⁻²⁷ in view of the d -electrons, local Coulomb and Hund's rule interactions in the iron pnictides, as opposed to the itinerant RPA-type treatment. Of them the so-called J_1 - J_2 model which emphasizes the As-bridged superexchange couplings^{22,28,29} between the nearest neighboring (NN) and next nearest neighboring (NNN) local moments of the irons has been used due to its natural tendency to form the collinear AF order at low temperature. The local moment approach is especially appealing over the itinerant one in explaining the

anomalous large linear-temperature susceptibility in the normal state over a wide temperature regime²⁷. However, how this localized spin picture can be meaningfully applied to a metallic material (albeit a bad metal in the undoped case of the iron-pnictides) remains unclear. Whether the doping effect is similar to that of the cuprates as described by a multiband t - J_1 - J_2 like model is also controversial.

In this paper, we point out that if *both* itinerant electrons and local moments are allowed to simultaneously present in the system, then many basic properties of the iron pnictides can be naturally accommodated by a single framework in the leading order approximation. To illustrate the point, we study a highly simplified model with the local moments and itinerant electrons coupled together by a Hund's rule coupling as schematically illustrated in Fig. 1. We show that an SDW order of the itinerant electrons can take place simultaneously with a collinear AF order of the local moments, while the ordering would be absent in either degrees of freedom if they do not couple, clearly different from the Fermi surface nesting mechanism or the AF ordering in a J_1 - J_2 model. Furthermore, the superconducting pairing of the itinerant electrons is also driven by the same coupling with the strength reaching strong coupling. Such a picture is further supported by a series of magnetic properties both below and above the SDW ordering temperature T_{SDW} , which show good agreement with experiments. It is predicted that in order to consistently account for T_{SDW} , magnetization, spin gap, uniform susceptibility, as well as the competition between the AF and SC phases, the (high-temperature) normal state of local moments should be close to a critical regime of quantum magnets, which can be tested by a neutron-scattering experiment.

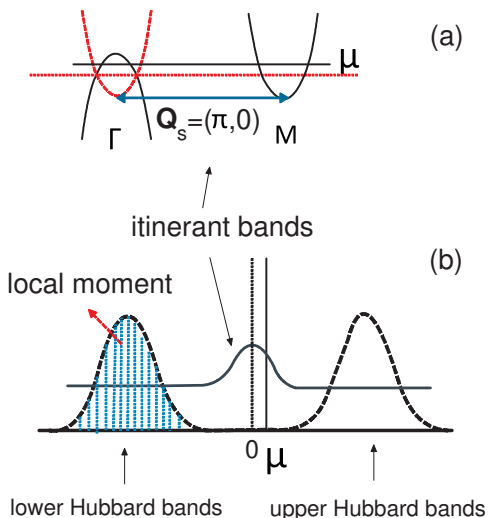


FIG. 1: (color online) A schematic illustration of itinerant electron and local moment bands and the profiles of density of states in the present model. (a) A simplified picture of two itinerant bands: A hole-like band near Γ point and an electron-like one near M point, which are separated by a moment $\mathbf{Q}_s = (\pi, 0)$; (b) The density of states for the itinerant bands shows an enhancement at chemical potential μ near the origin where both the hole and electron pockets contribute (see (a)); The local moment as an independent degrees of freedom is contributed by a filled lower Hubbard band, with the Mott gap crossing the Fermi level such that it does not contribute to the low-energy charge dynamics. The Hund's rule coupling between the itinerant electrons at the Fermi level and the local moments will dictate the low-energy physics.

II. MODEL STUDY

A. Minimal model

Our model Hamiltonian is composed of three terms

$$H = H_{\text{it}} + H_{J_0} + H_{J_2}. \quad (1)$$

The first term

$$H_{\text{it}} = \sum_{\mathbf{k}, \sigma} (\varepsilon_{\mathbf{k}} - \mu) c_{\mathbf{k}\sigma}^\dagger c_{\mathbf{k}\sigma} \quad (2)$$

describes the itinerant electrons forming the hole and electron pockets near the Fermi energy as illustrated in Fig. 1(a), which are located at the Γ point and the M point, respectively, and separated by momenta $\mathbf{Q}_s = (\pi, 0)$ and $(0, \pi)$ [only the former is shown in Fig. 1(a)] in an extended Brillouin zone (BZ). For simplicity we shall assume the symmetric dispersions for the hole and electron bands, with $\varepsilon_{\mathbf{k}} = -\varepsilon_{\mathbf{k}+\mathbf{Q}_s}$ such that the hole and electron pockets are exactly nested at $\varepsilon_{\mathbf{k}} = \mu = 0$, where μ is the chemical potential. Such nesting of the Fermi pockets will be lifted as the increase (decrease) of μ , which effectively controls the electron (hole) doping (the undoped case in iron pnictides may correspond to some small but finite $|\mu|$ here).

In contrast to the conventional itinerant approach where the Coulomb interaction between the itinerant electrons gets enhanced via the Fermi surface nesting effect, we shall omit such an interaction. Instead, we emphasize the importance of the coupling between the itinerant electrons and some preformed local moments via the second term H_{J_0} in (1), by a renormalized Hund's rule coupling J_0 as follows

$$H_{J_0} = -J_0 \sum_i \mathbf{M}_i \cdot \mathbf{S}_i \quad (3)$$

where \mathbf{S}_i is the spin operator for the itinerant electrons and \mathbf{M}_i denotes the local moment at site i . In the following we shall focus on the weak J_0 case where \mathbf{M}_i behaves like an independent degree of freedom. In the strong coupling limit of J_0 , by contrast, \mathbf{S}_i and \mathbf{M}_i should be locked together in strongly correlated regime as has been previously discussed in Ref.²³.

An essential assumption of this model will be that besides the itinerant electrons described above, there are some d -electrons sitting *below* the Fermi energy that can also contribute to the low-energy physics by forming effective local magnetic moments²³. Namely, some of the d -electron multibands can open up a Mott-Hubbard gap crossing the Fermi energy, due to the on-site Coulomb interaction and the Hund's rule ferromagnetic (FM) coupling, with the filled lower Hubbard bands giving rise to an effective local moment as illustrated in Fig. 1(b). These localized d -electrons may be different from the itinerant electrons as mainly coming from more isolated³¹ $d_{x^2-y^2}$ and d_{z^2} orbitals. In the following we shall simply assume their existence and explore the consequences of it.

The third term in (1) describes the predominant interaction between these local moments by a Heisenberg-like model

$$H_{J_2} = J_2 \sum_{\langle ij \rangle \in A} \mathbf{M}_i \cdot \mathbf{M}_j + J_2 \sum_{\langle ij \rangle \in B} \mathbf{M}_i \cdot \mathbf{M}_j \quad (4)$$

where the NNN superexchange coupling J_2 is bridged by the As ions between the diagonal iron sites, with A and B referring to two sublattices of the square Fe ion lattice, according to the LDA calculation^{28,29} and analysis²². Note that the NN exchange J_1 , bridged by the As ions, can be either AF or FM in nature and much weaker than J_2 for the isolated $d_{x^2-y^2}$ and d_{z^2} orbitals due to the symmetry reason^{22,31,32}. Furthermore, the itinerant electrons can effectively induce an additional NN FM interaction between the local moments, which is assumed to be predominant (to be consistent with the lattice distortion induced by the SDW ordering observed in the neutron scattering measurement^{6,8}, see below). Thus we shall neglect the effect of J_1 to the leading order approximation. Of course, one may always add such J_1 term as well as the Coulomb interaction between the itinerant electrons into the above highly simplified model to make it more realistic. But for the purpose of identifying

the most essential components and the simplicity of the model, we shall focus on the minimal model (1) in the following study.

B. Mean field approximation

1. Effective description of the local moments

According to (4), the local moments \mathbf{M}_i will antiferromagnetically fluctuate in each *sublattice* of the iron square lattice, and thus may be redefined by $\mathbf{M}_i \equiv Mp_i\mathbf{n}_i$ with $p_i \equiv e^{i\mathbf{Q}_s \cdot \mathbf{r}_i}$ with $\mathbf{Q}_s = (\pi, 0)$ and $(0, \pi)$ such that the unit vector \mathbf{n}_i will fluctuate smoothly in each sublattice. For the iron pnictides, the presence of the Mott-Hubbard gap is not expected to be very large (~ 0.6 eV as indicated in the optical experiment³⁰). It is enough to *protect* the local moments from amplitude fluctuations over a wide temperature regime presumably much higher than the SDW ordering temperature T_{SDW} as well as T_c . But it also means that in reality the local moment M is not quantized and described by a Heisenberg-like Hamiltonian (with $S = 2$ for instance).

Thus it would be more suitable to use a nonlinear σ -model^{33,34} to characterize the low-energy fluctuations of local moments in replace of (4):

$$\mathcal{L}_{J_2} = \sum_{a=A,B} \left\{ \frac{1}{2g_0} [(\partial_\tau \mathbf{n}_a)^2 + c^2(\nabla_{\mathbf{r}} \mathbf{n}_a)^2 + i\lambda_a(\mathbf{n}_a^2 - 1)] \right\} \quad (5)$$

with $c \simeq 4MJ_2$ (with the lattice constant of the Fe square lattice taking as the unit) and $g_0 \simeq 16J_2$. (Note that \mathbf{n}_a ($a = A, B$) here denotes the unit vector in a given sublattice such that two *separated* Néel orders would emerge, if $\lambda_a = 0$ at $T = 0$.) Denoting $\mathbf{n}_0 \equiv \langle \mathbf{n}_a \rangle$, the fluctuations of $\delta \mathbf{n} \equiv \mathbf{n} - \mathbf{n}_0$ is described by the propagator $D_0(\mathbf{q}, \tau) = -\langle T_\tau \delta \mathbf{n}(\mathbf{q}, \tau) \cdot \delta \mathbf{n}(-\mathbf{q}, 0) \rangle$ with^{33,34}

$$D_0(\mathbf{q}, i\omega_n) = -\frac{3g_0}{\omega_n^2 + \Omega_{\mathbf{q}}^2} \quad (6)$$

where the spin-wave spectrum

$$\Omega_{\mathbf{q}} = \sqrt{c^2 \mathbf{q}^2 + \eta^2} \quad (7)$$

and $\eta^2 \equiv i\lambda_a$ with the subscription a being dropped, which is determined by the condition $\langle (\mathbf{n}_a)^2 \rangle = 1$ as

$$(\mathbf{n}_0)^2 - \beta^{-1} \sum_{\omega_n, \mathbf{q} \neq 0} D_0(\mathbf{q}, i\omega_n) = 1 \quad (8)$$

with $\beta \equiv 1/k_B T$ and $\omega_n = 2\pi n\beta$. Hence, without coupling to the itinerant electrons, \mathbf{n}_a ($a = A, B$) do not couple to one another, and the local moment \mathbf{M}_i governed by (5) will intrinsically fluctuate around the two possible \mathbf{Q}_s 's.

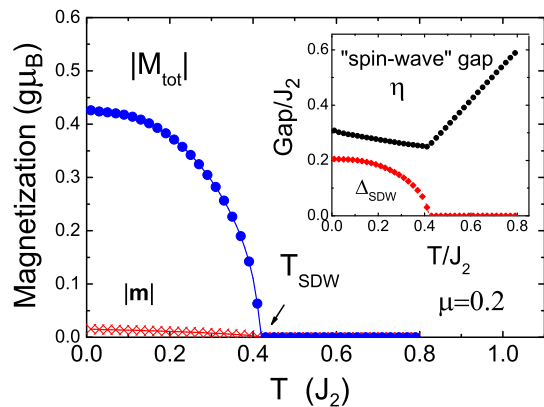


FIG. 2: (color online) The total magnetization and the induced moment of itinerant electrons at a fixed chemical potential $\mu = 0.2J_2$. Inset: the gaps in the “spin wave” spectrum $\Omega_{\mathbf{q}}$ of local moments and the SDW spectrum $E_{\mathbf{k}}$ of itinerant electrons.

2. Mean-field theory

It is important to note that such fluctuations will strongly couple to itinerant electrons via H_{J_0} , for the hole Fermi pockets around the Γ point and electron Fermi pockets around the M point are approximately connected by the momentum \mathbf{Q}_s at small μ , as shown in Fig. 1(a). In particular, driven by H_{J_0} , the local moments and particle-hole pairs can simultaneously condense at a specific wavevector \mathbf{Q}_s , giving rise to an AF order at a finite mean-field temperature T_{SDW} , which can be stabilized presumably by a weak interlayer coupling.

Assume an SDW order parameter for the itinerant electrons

$$\langle \mathbf{S}_i \rangle = \mathbf{m} p_i \neq 0 \quad (9)$$

with a specific wavevector $\mathbf{Q}_s = (\pi, 0)$ in $p_i \equiv e^{i\mathbf{Q}_s \cdot \mathbf{r}_i}$. Then a staggered “easy-axis field” from H_{J_0} should be added to the nonlinear σ -model in (5):

$$-J_0 M \mathbf{m} \cdot \sum_i \mathbf{n}_i. \quad (10)$$

The resulting Euclidean action is still quadratic in \mathbf{n}_i and can be integrated out in a standard way to give rise to the same expressions of (6) and (8), except that now \mathbf{n}_0 is determined by

$$\begin{aligned} \mathbf{n}_0 &\equiv \langle \mathbf{n}_a \rangle \\ &= (J_0 M g_0 / \eta^2) \mathbf{m}. \end{aligned} \quad (11)$$

Thus, no matter how weak \mathbf{m} is, it can always induce a collinear AF order of the local moments at the same \mathbf{Q}_s with $\mathbf{n}_0 \neq 0$. In particular, the independent spin wave spectrum $\Omega_{\mathbf{q}}$ of the local moment gains a finite gap $\eta \neq 0$, in contrast to the limit of $\mathbf{m} = 0$ where $\mathbf{n}_0 \neq 0$ can only occur at $\eta = 0$ in a pure J_2 nonlinear σ -model^{33,34}.

Self-consistently, with $\mathbf{n}_0 \neq 0$ a finite \mathbf{m} will always be induced in the itinerant electrons. At the mean-field level, it is governed by

$$H_{\text{it}} - J_0 M \mathbf{n}_0 \cdot \sum_i p_i \mathbf{S}_i, \quad (12)$$

leading to the following band folding and reconstruction

$$\sum'_{\mathbf{k}, \sigma} \left[(-E_{\mathbf{k}} - \mu) \alpha_{\mathbf{k}\sigma}^\dagger \alpha_{\mathbf{k}\sigma} + (E_{\mathbf{k}} - \mu) \beta_{\mathbf{k}\sigma}^\dagger \beta_{\mathbf{k}\sigma} \right] \quad (13)$$

where the summation over \mathbf{k} is restricted within the reduced magnetic BZ defined by \mathbf{Q}_s and the itinerant electron bands are split into α and β bands, with the Bogoliubov transformation

$$\begin{aligned} c_{\mathbf{k}\sigma} &= u_{\mathbf{k}} \alpha_{\mathbf{k}\sigma} - v_{\mathbf{k}} \sigma \beta_{\mathbf{k}\sigma}, \\ c_{\mathbf{k}+\mathbf{Q}_s\sigma} &= v_{\mathbf{k}} \sigma \alpha_{\mathbf{k}\sigma} + u_{\mathbf{k}} \beta_{\mathbf{k}\sigma}. \end{aligned} \quad (14)$$

Here $u_{\mathbf{k}} = [(1 - \epsilon_{\mathbf{k}}/E_{\mathbf{k}})/2]^{1/2}$, $v_{\mathbf{k}} = [(1 + \epsilon_{\mathbf{k}}/E_{\mathbf{k}})/2]^{1/2}$, and the electron excitation spectrum becomes

$$E_{\mathbf{k}} = \sqrt{\epsilon_{\mathbf{k}}^2 + \Delta_{\text{SDW}}^2} \quad (15)$$

in which the SDW gap

$$\Delta_{\text{SDW}} \equiv \frac{J_0 M}{2} |\mathbf{n}_0|. \quad (16)$$

Finally, the self-consistent mean-field equation reads

$$|\mathbf{m}| = \frac{\Delta_{\text{SDW}}}{N} \sum'_{\mathbf{k}} \frac{1}{E_{\mathbf{k}}} (n_{\mathbf{k}\alpha} - n_{\mathbf{k}\beta}), \quad (17)$$

where $n_{\mathbf{k}\alpha} = 1/(e^{-\beta(E_{\mathbf{k}}+\mu)} + 1)$ and $n_{\mathbf{k}\beta} = 1/(e^{\beta(E_{\mathbf{k}}-\mu)} + 1)$.

C. Physical properties

1. Mean-field results

Solving the above mean-field equations, one can determine T_{SDW} for the collinear AF order and the total magnetization defined by

$$\mathbf{M}_{\text{tot}} \equiv g\mu_B (M\mathbf{n}_0 + \mathbf{m}), \quad (18)$$

($g = 2$). The results are shown in Fig. 2. Here we have fixed the parameters $M = 0.8$ and $J_0 = J_2$ throughout the paper, with J_2 tunable. The hole dispersion of the itinerant electrons is parameterized as $\epsilon_{\mathbf{k}} = -\alpha(\mathbf{k}^2 - k_0^2)$ with $\alpha = 7J_2$ and $k_0 = 0.1\pi$ based on the ARPES measurement for the so-called ‘‘122-type’’ BaFe_2As_2 ^{35–38}.

It is noted that the above choice of the parameters is not necessarily optimized. But such a set of parameters can give rise to a quantitative account of a series of important experimental results. The calculated $|\mathbf{M}_{\text{tot}}| \simeq 0.85 \mu_B$ at $T = 0$ (which is independent of J_2

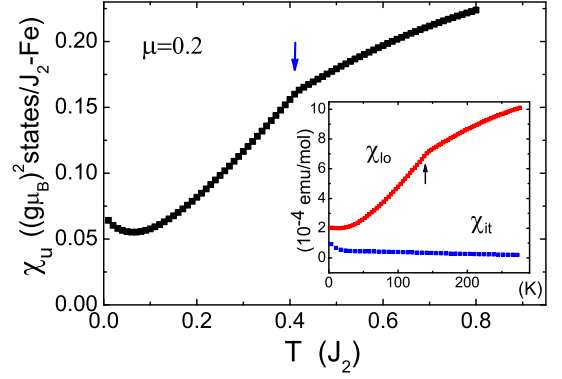


FIG. 3: (color online) The calculated uniform spin susceptibility χ_u shows a linear-T behavior above T_{SDW} (marked by arrow) using the same set of parameters as used in Fig. 2. Inset: The susceptibility χ_{lo} contributed by the local moments and χ_{it} from the itinerant electrons are illustrated separately, in absolute units comparable to the experimental data with taking $J_2 = 30$ meV.

as shown in Fig. 2) is close to $0.87 \mu_B$ for BaFe_2As_2 ^{8,11}. By taking $J_2 = 30$ meV (incidentally it is comparable to the LDA estimation²⁹ for BaFe_2As_2), one obtains $T_{\text{SDW}} \simeq 0.415J_2 = 144$ K (compared to the experimental value 143 K⁸), and in the inset of Fig. 2, a gap $\eta = 0.31J_2 = 9.3$ meV opened up in the spin wave spectrum of the local moments is also fairly close to the experimental value 9.8 meV¹¹ (a similar fit for SrFe_2As_2 ¹⁰ can be also obtained). Note that a proper cut-off momentum $\Lambda = 0.225\pi$ is taken in solving (8) and its role in general will be discussed later together with the comparison with other materials.

2. Uniform magnetic susceptibility

Using the same set of parameters, the uniform susceptibility

$$\chi_u = \chi_{\text{lo}} + \chi_{\text{it}} \quad (19)$$

is calculated and presented in Fig. 3, which exhibits a pseudogap behavior below T_{SDW} and a rough linear-temperature dependence in the normal state, mainly due to the contribution χ_{lo} from the local moments as shown in the inset. As indicated in the latter, both the magnitude and slope of χ_{lo} are also quantitatively comparable to the experimental measurements^{27,39,40}. Here χ_{lo} is given by³⁴

$$\chi_{\text{lo}} = \frac{2}{3} \chi_{\perp} \mathbf{n}_0^2 + 2\beta^{-1} \sum_{\omega_n, \mathbf{q}} \frac{-\omega_n^2 + c^2 \mathbf{q}^2 + \eta^2}{(\omega_n^2 + c^2 \mathbf{q}^2 + \eta^2)^2} \quad (20)$$

in units of $(g\mu_B)^2$ where $\chi_{\perp} = 1/g_0$.

The contribution from the itinerant electrons is given by

$$\chi_{\text{it}} = \frac{\beta}{2N} \sum'_{\mathbf{k}} [n_{\mathbf{k}\alpha} (1 - n_{\mathbf{k}\alpha}) + n_{\mathbf{k}\beta} (1 - n_{\mathbf{k}\beta})] \quad (21)$$

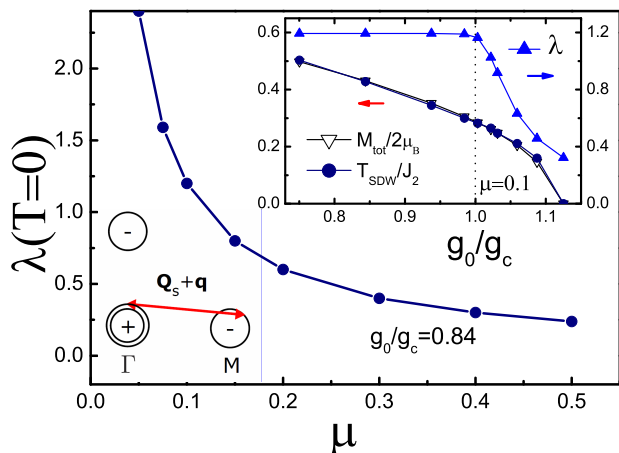


FIG. 4: (color online) The pairing strength λ vs. μ , with the relative sign change of the pair amplitude shown at the left bottom. Inset: Variations of λ , M_{tot} , and T_{SDW} vs. the parameter g_0/g_c of the nonlinear σ -model (5) (see text).

in units of $(g\mu_B)^2$. χ_{it} is mostly Pauli-like, except for an upturn at low temperature as shown in the inset of Fig. 3, which is due to the enhanced density of states in the induced SDW state where the SDW gap is near but not right at the Fermi level. It results in the upturn of the total susceptibility at low temperature as shown in Fig. 3.

Thus, the present theory not only gives rise to the large, linear-temperature dependent susceptibility above T_{SDW} , but also naturally explains the quick drop of the susceptibility below T_{SDW} due to the gap opening and its upturn at even lower temperatures generically found in the iron pnictides^{39,40}.

3. Pairing strength

The itinerant electrons can also exchange the quantum fluctuations of the local moments to form Cooper pairs, which resonantly hop between the electron and hole pockets with large momentum transfers around \mathbf{Q}_s . The pairing amplitude is s-wave within each Fermi pocket, but has to change *sign* between the two pockets due to exchanging the spin fluctuation D_0 [(6)], consistent with other approaches^{15,16,21,25} and measurement³⁷.

In Fig. 4, an effective dimensionless pairing strength λ as function of μ is calculated based on the same set of parameters with fixing $\mathbf{m} = 0$, i.e, in the absence of the SDW order. Here λ is given by

$$\lambda \equiv 2 (J_0 M)^2 N_F \langle (-1) D_0(\mathbf{k} - \mathbf{k}' - \mathbf{Q}_s, \omega = 0) \rangle_{\text{FS}} \quad (22)$$

where $N_F = 1/(4\pi\alpha)$ denotes the density of states at the Fermi energy and the average is over the Fermi pockets. Note that to properly estimate the strength we have considered two hole pockets at Γ and two electron pocket at two M 's in consistency with ARPES experiments³⁷,

as marked in the left bottom in Fig. 4, where the sign change of the pairing amplitude is also indicated. The main panel of Fig. 4 shows that λ is fairly large in a wide regime (it even diverges at $\mu = 0$ due to the artificial nesting effect of the Fermi pockets). Thus the superconducting phase is expected to strongly compete with the SDW state at low doping.

We further find that M_{tot} and T_{SDW} are quite flat as function of μ , insensitive to doping. But the SDW order is very sensitive to the aforementioned momentum cut-off Λ , which decides the critical coupling constant³³ $g_c = 4\pi c/3\Lambda$ in the nonlinear σ -model (5). Indeed, as given in the inset of Fig. 4, both M_{tot} and T_{SDW} are well scaled together and monotonically decrease with the increase of $g_0/g_c \propto \Lambda$, whereas λ remains flat until reaching beyond $g_0/g_c = 1$ (on the right hand side of the dashed vertical line). A quantitative check reveals that a good agreement with experiments always occurs in the regime that the coupling constant g_0 is not far from the quantum critical point g_c . For instance, by increasing Λ , say, to $g_0/g_c \simeq 1.03$, $|M_{\text{tot}}|$ reduces to $0.42 \mu_B$ and $T_{\text{SDW}} \simeq 0.2J_2 = 139$ K by choosing $J_2 = 60$ meV. Then one can get a good quantitative account for the similar properties of the so-called “1111” compounds^{6,9}, like LaOFeAs. Note that as compared to the “122” materials the J_2 value here is doubled, which is also comparable to the LDA estimation²⁹ for LaOFeAs. Using the BCS formula

$$T_c \simeq \omega_0 \exp[-(1 + \lambda)/\lambda], \quad (23)$$

it explains why T_c can be much higher in the “1111” compounds⁵ as $\omega_0 \propto J_2$.

Furthermore, since $\omega_0 \propto J_2$, one can estimate the isotope effect of the iron mass based on

$$J_2 \propto 1 + \langle |u|^2 \rangle \quad (24)$$

(using the fact that the effective hopping integral $\propto 1 + u$ under a relative lattice displacement u) and $\langle |u|^2 \rangle \propto 1/(M_{\text{Fe}}\Theta_D) \propto (M_{\text{Fe}})^{-1/2}$ as in the Debye-Waller factor (Θ_D is the Debye frequency and M_{Fe} the iron mass), with

$$\alpha_{\text{SC}} \equiv -d \ln T_c / d \ln M_{\text{Fe}} \simeq 0.5 \left[\langle |u|^2 \rangle / (1 + \langle |u|^2 \rangle) \right]. \quad (25)$$

According to the inset of Fig. 4, $T_{\text{SDW}} \propto J_2$ and thus the magnetic isotope coefficient $\alpha_{\text{SDW}} \equiv -d \ln T_{\text{SDW}} / d \ln M_{\text{Fe}}$ is related to α_{SC} by

$$\alpha_{\text{SDW}} \simeq \alpha_{\text{SC}} \quad (26)$$

which is consistent with the recent experimental result⁴², but the positive α_{SC} here is in contrast with another recent experiment⁴³ where a negative α_{SC} is obtained for samples of high-pressure synthesis. Whether the isotope effect is positive or negative needs a further experimental clarification.

III. CONCLUSION AND DISCUSSION

In this paper, we have proposed a minimal model based on some basic band-structure and experimental facts, and shown that it can provide a systematic and quantitative account for a series of anomalous magnetic and SC properties observed in the iron pnictides.

This is a multiband model, composed of two independent and distinct components, i.e., the itinerant electrons and local moments, respectively. Here the charge carriers of the itinerant bands presumably come from the more extended d -orbitals, like d_{xy} , d_{zx} , and d_{yz} . The local moments are contributed by the electrons from some more localized orbitals, say, $d_{x^2-y^2}$ and d_{z^2} orbitals, forming at much higher temperature than that of the SDW ordering observed in the experiment. Such local moments are protected by a Mott gap which is supposed to cross the Fermi level all the time such that they do not directly contribute to the charge dynamics. Finally the two independent degrees of freedom, the itinerant electrons and local moments, are coupled together by the local Hund's rule interaction inside each iron.

This is a highly simplified model. We have totally omitted the Coulomb interaction between the itinerant electrons such that the SDW ordering of the itinerant electrons is not driven by a conventional picture of Fermi surface nesting effect. For the local moments from the $d_{x^2-y^2}$ and/or d_{z^2} orbitals, we have only kept the dominant NNN J_2 superexchange coupling, bridged by the As ions, and neglected the NN coupling J_1 due to the symmetry reason. So the local moments alone do not form the proper collinear AF order as seen in experiment, and are effectively described by the familiar NNN AF nonlinear σ -models at two sublattices, respectively.

Then we have shown that the magnetic ordering can be simply realized due to the strong Hund's rule coupling between the two components. Namely the itinerant electrons can form an SDW order simultaneously with the collinear AF order of the local moments at the same momentum \mathbf{Q}_s below a mean-field transition temperature T_{SDW} , with H_{J_0} gaining a mean-field energy.

Of course, one may further consider the Coulomb interaction in the itinerant bands which may result in an SDW instability without involving the local moments. Or one can further introduce the NN coupling J_1 for the local moments and obtain a collinear AF state independent of the itinerant electrons. But the key assumption in this approach is that these effects are negligible, to the leading order approximation, as compared to the Hund's rule coupling term and thus are omitted for simplicity. One can always make the model more realistic by adding more perturbative terms later. As a matter of fact, in the experimentally observed lattice distortion^{6,8} accompanying the collinear AF order, the NN spins along the shorter lattice constant direction are always FM parallel while the antiparallel NN spins usually correspond to the longer lattice constant⁸, in contrast to a J_1 -driven mechanism which would prefer an opposite lattice distortion²⁴.

This provides a further support for the mechanism of the Hund's rule coupling, with the FM spins at the shorter NN sites in favor of the kinetic energy of the itinerant electrons.

Therefore, it is the Hund's rule coupling term (3) that makes the present minimal model nontrivial. By locking the SDW order of the itinerant electrons and local moments together at the wavevector \mathbf{Q}_s , an imperfect "nesting" of the hole and electron pockets by \mathbf{Q}_s and the short-range AF ordering of the local moments at \mathbf{Q}_s are synchronized to optimize the total energy. One finds that T_{SDW} , the magnitude of the total magnetization moment, the small spin gap due to the out-of-phase relative fluctuations of the SDW moments between the itinerant electrons and local moments, can be quantitatively determined, in good agreement with the experimental results.

Compared to the conventional Fermi surface nesting mechanism for the itinerant electrons, the present model naturally predicts the presence of pre-formed magnetic moments above the SDW ordering temperature. The calculated normal-state magnetic susceptibility above T_{SDW} shows a linear-temperature behavior consistent with the experiment in magnitude and slope, under the same set of parameters, which is difficult to understand by the itinerant electrons alone. Furthermore, while the Fermi surface nesting mechanism is difficult to explain why T_c is so high in the iron pnictides, the computed pairing strength between the itinerant electrons via exchanging the AF fluctuations of the local moments is found to be easily in strong coupling regime in the present work, using the same parameters.

On the other hand, as compared to a conventional J_1 - J_2 model where the collinear AF transition can occur alone at low temperature, in the present model the itinerant electrons play a crucial role in driving the magnetic ordering by coupling to the local moments, and by doing so drastically change their own dynamics below T_{SDW} , resulting in peculiar gap behaviors in static and dynamic susceptibilities as well as the scattering rate change in optical conductivity, which have been observed experimentally and are hard to understand if the magnetic ordering is due to the J_1 - J_2 superexchange interaction alone.

As a matter of fact, in order to provide a consistent explanation of some generic phenomena found in the iron pnictides including the SDW and SC orders within a single framework, the present model predicts that in the normal state the local moments should be close to a critical regime of quantum magnets with the dominant J_2 -type superexchange interaction, which can be critically tested by a neutron-scattering experiment. The magnetic state of the local moments is also expected to play an important role in the superconducting state. Here the reason behind the rise of T_c by doping or pressure in experiment may be not due to a pure increase of charge carrier number like in the cuprates, but rather due to the suppression of the collinear AF order in favor of superconductivity, as the result of the accompanying change in the ratio g_0/g_c near the quantum critical regime^{33,41}, as discussed above.

However, how this mechanism can be realized microscopically is beyond the scope of the present work, which may involve detailed and realistic local interactions (including J_1), and will be left for a future study.

Acknowledgments

We would like to acknowledge stimulating discussions with D.H. Lee, Z.Y. Lu, Q.H. Wang, Y.Y. Wang, M.Q.

Weng, M.W. Wu, T. Xiang, J. Zaanen, G.M. Zhang, and also thank W. Bao, X.H. Chen, P. C. Dai, H. Ding, D.L. Feng, N.L. Wang, H.H. Wen, and X. J. Zhou for generously sharing their experimental results. This work is supported by NSFC, NBRPC, and NCET grants.

-
- * Electronic address: weng@tsinghua.edu.cn
- ¹ Y. Kamihara, *et al.*, J. Am. Chem. Soc. **128**, 10012 (2006); Y. Kamihara, *et al.*, J. Am. Chem. Soc. **130**, 3296 (2008).
 - ² H.-H. Wen, *et al.*, Europhys. Lett. **82**, 17009 (2008).
 - ³ X. H. Chen, *et al.*, Nature (London) **453**, 761 (2008).
 - ⁴ G. F. Chen, *et al.*, Phys. Rev. Lett. **100**, 247002 (2008).
 - ⁵ Z.A. Ren, *et al.*, Europhys. Lett. **83**, 17002 (2008).
 - ⁶ C. de la Cruz, *et al.*, Nature (London) **453**, 899 (2008).
 - ⁷ M. A. McGuire, *et al.*, Phys. Rev. B **78**, 094517 (2008).
 - ⁸ Q. Huang, *et al.*, Phys. Rev. Lett. **101**, 257003 (2008).
 - ⁹ Y. Chen, *et al.*, Phys. Rev. B **78**, 064515 (2008).
 - ¹⁰ J. Zhao, *et al.*, Phys. Rev. Lett. **101**, 167203 (2008).
 - ¹¹ K. Matan, *et al.*, Phys. Rev. B **79**, 054526 (2009).
 - ¹² J. Dong, *et al.*, Europhys. Lett. **83**, 27006 (2008).
 - ¹³ C. Cao, *et al.*, Phys. Rev. B **77**, 220506 (R) (2008).
 - ¹⁴ D. J. Singh and M. H. Du, Phys. Rev. Lett. **100**, 237003 (2008).
 - ¹⁵ I. Mazin, *et al.*, Phys. Rev. Lett. **101**, 057003 (2008).
 - ¹⁶ K. Kuroki, *et al.*, Phys. Rev. Lett. **101**, 087004 (2008).
 - ¹⁷ Q. Han, *et al.*, Europhys. Lett. **82**, 37007 (2008); Z. J. Yao, *et al.*, New J. Phys. **11**, 025009 (2009).
 - ¹⁸ T. Li, *et al.*, J. Phys: Condens. Matter **20**, 425203 (2008).
 - ¹⁹ S. Raghu, *et al.*, Phys. Rev. B **77**, 220503 (2008); X.L. Qi, *et al.*, arXiv:0804.4332 (unpublished).
 - ²⁰ P. A. Lee and X. G. Wen, Phys. Rev. B **78**, 144517 (2008).
 - ²¹ F. Wang, *et al.*, Phys. Rev. Lett. **102**, 047005 (2009); H. Zhai, *et al.*, Europhys. Lett. **85**, 37005 (2009).
 - ²² Q. Si and E. Abrahams, Phys. Rev. Lett. **101**, 076401 (2008).
 - ²³ Z. Y. Weng, arXiv:0804.3228.
 - ²⁴ C. Xu, *et al.*, Phys. Rev. B **78**, 020501 (R) (2008).
 - ²⁵ C. Fang, *et al.*, Phys. Rev. B **77**, 224509 (2008); K. Seo, *et al.*, Phys. Rev. Lett. **101**, 206404 (2008).
 - ²⁶ W. Q. Chen, *et al.*, Phys. Rev. Lett. **102**, 047006 (2009).
 - ²⁷ G. M. Zhang, *et al.*, arXiv:0809.3874 (unpublished).
 - ²⁸ T. Yildirim, Phys. Rev. Lett. **101**, 057010 (2008).
 - ²⁹ F. Ma, *et al.*, Phys. Rev. **78**, 224517 (2008).
 - ³⁰ W. Z. Hu, *et al.*, Phys. Rev. Lett. **101**, 257005 (2008).
 - ³¹ J. Wu, *et al.*, Phys. Rev. Lett. **101**, 126401 (2008).
 - ³² V. Cvetkovic and Z. Tesanovic, Europhys. Lett. **85**, 37002 (2009).
 - ³³ S. Chakravarty, *et al.*, Phys. Rev. B **39**, 2344 (1989).
 - ³⁴ S. Sachdev, *Quantum Phase Transitions*, Cambridge University Press (1999).
 - ³⁵ L. X. Yang, *et al.*, Phys. Rev. Lett. **102**, 107002 (2009).
 - ³⁶ C. Liu, *et al.*, Phys. Rev. Lett. **101**, 177005 (2008).
 - ³⁷ H. Ding *et al.*, Europhys. Lett. **83**, 47001 (2008).
 - ³⁸ H. Liu, *et al.*, Phys. Rev. B **78**, 184514 (2008).
 - ³⁹ X. F. Wang, *et al.*, Phys. Rev. Lett. **102**, 117005 (2009).
 - ⁴⁰ R. Klingeler, *et al.*, arXiv:0808.0708 (unpublished).
 - ⁴¹ S. Sachdev, *et al.*, Phys. Rev. B **51**, 14874 (1995).
 - ⁴² R. H. Liu, *et al.*, arXiv:0810.2694.
 - ⁴³ P. M. Shirage, *et al.*, arXiv:0903.3515 (unpublished).